Paper ID: 304

Optimization of Electron Transport Layer (ETL), Hole Transport Layer (HTL), and Absorber Material for Enhancing Efficiency of SnS-Based Solar Cells

Kristy Progya Biswas[1], Tabassum Fardous Nitu[2], Md. Nurul Islam[3]
[1, 2, 3] Department of Mechanical Engineering, Rajshahi University of Engineering & Technology, Rajshahi-6204, Bangladesh
E-mail: [1]*kristyprogya@gmail.com* , [2]*tabassumfardousnitu@gmail.com* , [3]*nurul93213@me.ruet.ac.bd*

Abstract

Solar cells play a pivotal role in the transition to renewable energy, offering a sustainable solution to the global energy crisis. However, achieving high efficiency and stability in photovoltaic devices remains a significant challenge. SnS-based solar cells emerge as a promising alternative due to their non-toxic, earth-abundant properties and stable amphoteric characteristics. This research addresses the critical gap in optimizing material combinations for SnS-based solar cells to enhance power conversion efficiency while maintaining stability. Using SCAPS-1D simulation software, this study evaluates and identifies optimal configurations for electron transport layers (ETLs), hole transport layers (HTLs), and absorber layers. The two best-performing structures, TCO/PCBM (ETL)/SnS/$CuSbS_2$ (HTL) and TCO/ZnO (ETL)/SnS/NiO (HTL), achieved power conversion efficiencies of 31.26% and 31.12%, respectively, demonstrating significant improvements over conventional designs. These findings provide a pathway for developing high-performance, stable SnS-based solar cells, potentially transforming their application in sustainable energy systems and advancing the photovoltaic industry.

Keywords: SnS-based solar cells, ETL, HTL, SCAPS-1D, Power conversion efficiency

1. Introduction

The significance of solar energy in the transition to clean, sustainable energy is becoming more widely acknowledged. This renewable power source provides reduced costs, along with low carbon emissions and pollution [1]. The development of extremely efficient polymer and perovskite solar cells has been a recent focus of many scholars; nevertheless, the instability of these technologies limits their long-term applicability. Thus, thin-film solar cells might be an excellent replacement for such approaches [2]. SnS has become a prominent absorber layer in thin-film solar cells due to its many benefits, one of which is its high absorption coefficient, which allows it to absorb a significant amount of the visible light spectrum. Moreover, SnS is an inexpensive and abundant mineral in the Earth [3]. With an energy band gap of 1.31 eV and a high absorption coefficient of 10^5 cm^-1, SnS offers a number of advantageous properties that enable SnS layers to effectively absorb a large amount of solar radiation [4]. In this study, two novel and extremely effective SnS-based solar cell structures have been designed through optimization: TCO/PCBM/SnS/$CuSbS_2$ and TCO/ZnO/SnS/NiO. Here, PCBM and ZnO are employed as the electron transport layers (ETLs), while $CuSbS_2$ and NiO are used as the hole transport layers (HTLs). In this assessment, transparent conductive oxide (TCO) plays a crucial role in these solar cells, facilitating efficient charge transport and enhancing overall device performance. The created cells are subjected to a numerical investigation employing SCAPS-1D software. The improved solar cells achieved a maximum efficiency of 31.26% and 31.12%, respectively. By optimizing the device architecture and enhancing light absorption, this research aims to establish a pathway for overcoming efficiency limitations in SnS-based thin-film solar cells, contributing to the development of stable and high-performance photovoltaic technologies.

2. Research methodology

The simulation software SCAPS-1D (Solar Cell Capacitance Simulator) was employed to conduct the numerical simulation. In this study, we explored the effects of different hole transport materials and electron transport materials on the properties of SnS-based solar cells, with particular emphasis on short-circuit current density (Jsc),

open-circuit voltage (Voc), fill factor (FF), and overall efficiency. These analyses were conducted by solving the fundamental equations of semiconductors [5].

This study employed PCBM and zinc oxide (ZnO) as electron transport materials, SnS as the active (or absorber) layer, and $CuSbS_2$ and NiO as hole transport materials. Using AM1.5G, simulations were conducted at a temperature of 300 K and an irradiance of 1000 W/m² under Standard Test Conditions (STC). To effectively simulate this solar cell, it is essential to provide a range of parameters related to the device's structure, materials, and physical properties. The physical input parameters that are required are displayed in Table 1.

Table 1. Properties of transparent conductive oxides (TCO), absorber material (SnS), electron transport materials (PCBM, ZnO) and hole transport materials ($CuSbS_2$) for the simulation.

Parameters	TCO [6]	SnS [7]	PCBM [8]	ZnO [9]	$CuSbS_2$ [10]	NiO [2]
Thickness(µm)	0.500	1.400	0.030	0.055	0.050	0.050
Bandgap(eV)	3.5	1.310	2.00	3.300	1.58	3.600
Electron affinity(eV)	4.00	4.200	3.900	4.00	4.200	2.10
Dielectric permittivity(relative)	9.00	13.000	4.00	9.00	14.6	11.75
Effective density of states of conduction band , $N_c(1/cm^3)$	2.00E+18	1.180E+18	1.00E+21	3.70E+21	2.00E+18	2.50E+20
Effective density of states of valence band , N_v $(1/cm^3)$	1.800E+19	4.760E+18	2.00E+20	1.80E+19	1.00E+18	2.500E+20
Electron mobility(cm^2/Vs)	2.00E+1	1.300E+2	1.00E-2	1.00E+2	4.90E+1	1.00E-3
Hole mobility (cm^2/Vs)	1.00E+1	4.300E+0	1.00E-2	2.50E+1	4.90E+1	1.00E-3
Acceptor density $(1/cm^3)$	0.00E+0	1.00E+15	0.00E+0	0.00E+0	1.00E+18	1.00E+19
Donor density $(1/cm^3)$	2.00E+19	0.00E+0	1.00E+20	1.00E+18	0.00E+0	5.00E+19
Total defect density, $N_t(1/cm^3)$	1.00E+15	1.00E+14	1.00E+14	1.00E+14	1.00E+14	1.00E+14

In the present investigation, the selection of SnS as the absorber layer was motivated by its non-toxic nature and superior optoelectronic characteristics. Many separate hole transport layers (HTLs), multiple distinct electron transport layers (ETLs), and SnS as the absorber layer were used in a variety of simulated scenarios. Out of the photovoltaic solar cell (PSC) models analyzed, the following two have been selected for optimization:

1. Right contact (front)/TCO/PCBM/SnS/$CuSbS_2$/Left contact (back)
2. Right contact (front)/TCO/ZnO/SnS/NiO/Left contact (back)

Model 1. Right contact (front) / PCBM / SnS / $CuSbS_2$ / Back contact (back) Influence of thickness and defect density on ETL (PCBM)

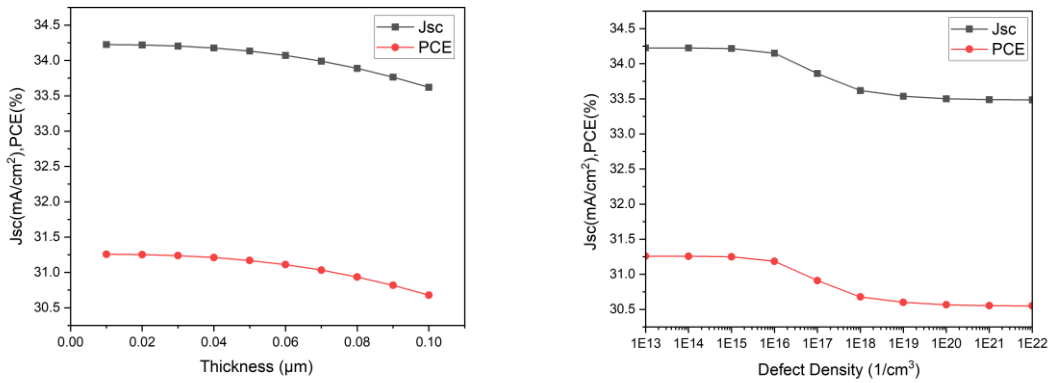


Fig. 1. Influence of thickness and defect density on ETL (PCBM)

In figure 1, it is found that the short-circuit current density (Jsc), and overall power conversion efficiency (PCE) all slightly decrease with increasing PCBM layer thickness. The maximum PCE value ever recorded, at a thickness of 0.01 µm, is 31.2573%.
Upon altering the defect density between 1.00E+13 cm^{-3} and 1.00E+22cm^{-3}, a synchronous drop in all performance parameters is seen. The highest percentage of PCE, at a defect density of 1.00E+13 cm^{-3}, is 31.2581 %.

Influence of thickness and defect density on absorber layer (SnS)

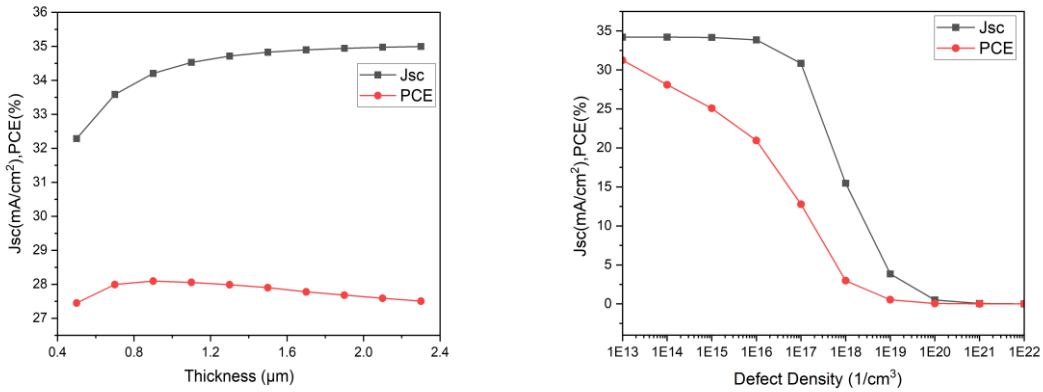


Fig. 2. Influence of thickness and defect density on absorber layer (SnS)
In figure 2, it is found that none of the performance measures significantly change when the absorber layer's thickness increases. A minor variation is observed when the thickness is altered. The maximum value of PCE is 27.4493 % at the thickness of 0.5 µm.
There are significant differences in the short-circuit current density (Jsc), and power conversion efficiency (PCE) depending on the defect density, which varies from 1.00E+13 cm^{-3} to 1.00E+22 cm^{-3}. The highest PCE value for a defect density of 1.00E+13 cm^{-3}, is 31.2376 %.

Influence of thickness and defect density on HTL ($CuSbS_2$)

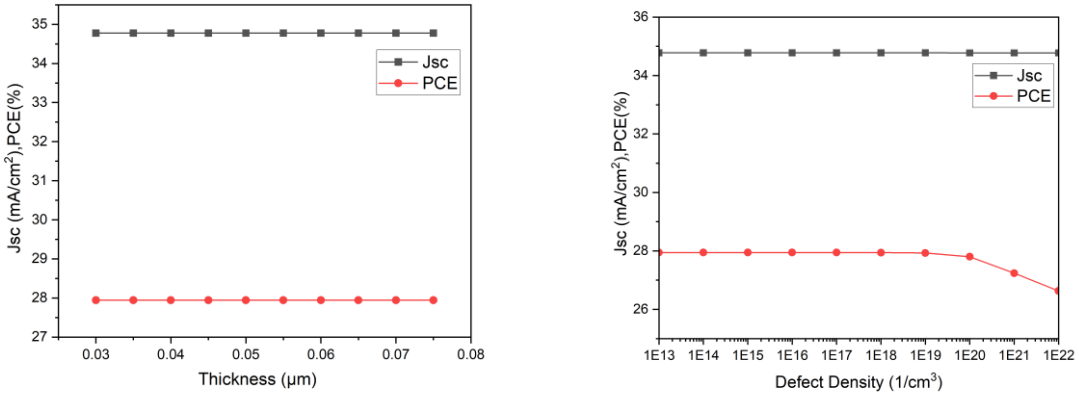


Fig. 3. Influence of thickness and defect density on HTL ($CuSbS_2$)
In figure 3, there is no significant increase in the values of Jsc, and PCE. The maximum value of PCE is 27.9443 % at the thickness of 0.03 µm.
As defect density rises, there is a notable decline in the short-circuit current density (Jsc), and power conversion efficiency (PCE). The peak PCE reaches 27.9446% and remains constant from 1.00E+13 cm^{-3} to 1.00E+16 cm^{-3}.

Model 2. Right contact (front)/TCO/ZnO/SnS/NiO/Left contact (back)
Influence of thickness and defect density on ETL (ZnO)

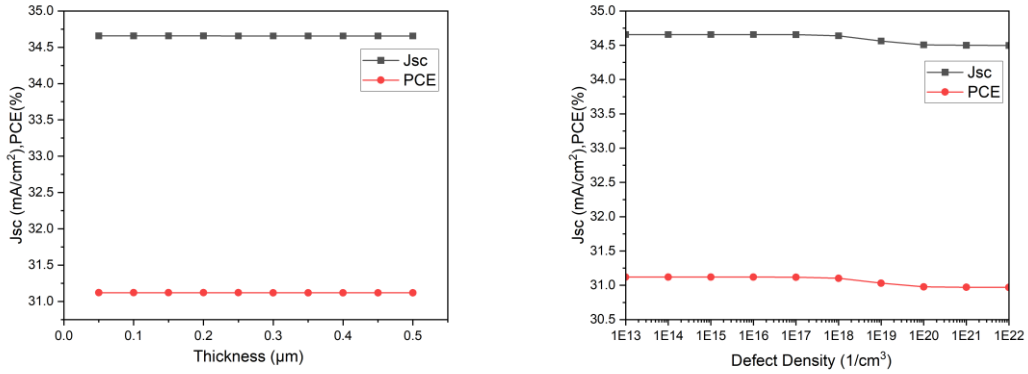


Fig. 4. Influence of thickness and defect density on ETL (ZnO)

In Figure 4, both the power conversion efficiency (PCE) and short-circuit current density (Jsc) show a negligible decline with increasing thickness. Additionally, only minimal variations in PCE and Jsc are observed as the defect density increases.

Influence of thickness and defect density on absorber layer (SnS)

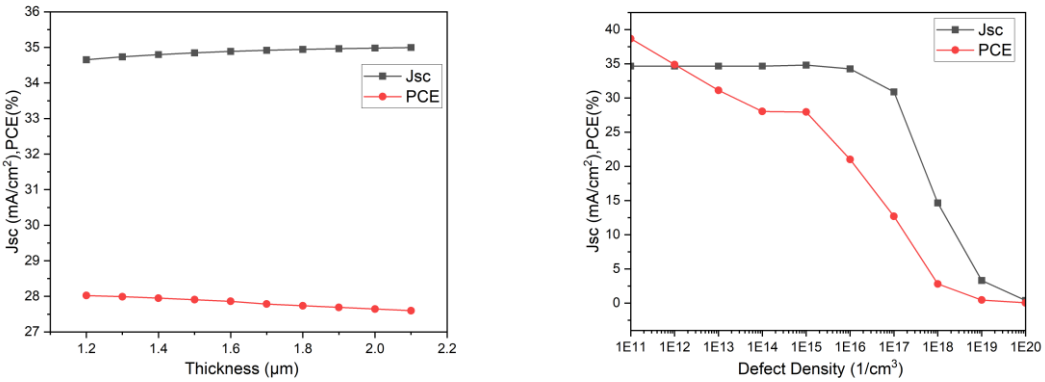


Fig. 5. Influence of thickness and defect density on absorber layer (SnS)

In figure 5, as the thickness rises, there is a slight reduction in the power conversion efficiency (PCE), accompanied by a small rise in the short-circuit current (Jsc). The peak PCE value of 28.0249% is achieved at a thickness of 1.2 μm.

Furthermore, an increase in defect density leads to a rapid decline in the short-circuit current (Jsc), and power conversion efficiency (PCE). The highest efficiency is achieved at a defect density of 1.00E+11 cm^{-3}.

Influence of thickness and defect density on HTL (NiO)

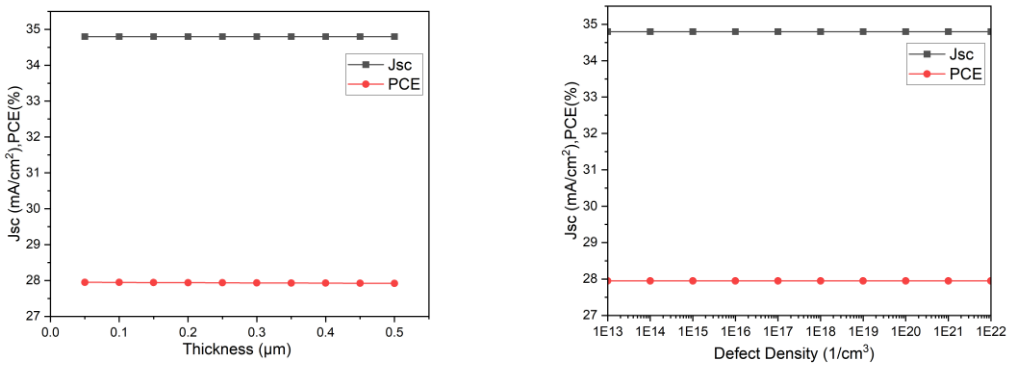


Fig. 6. Influence of thickness and defect density on HTL (NiO)

In figure 6, as the thickness increases, both the short-circuit current density (Jsc) and power conversion efficiency (PCE) exhibit a slight and nearly imperceptible decline.

The defect density in SnS-based solar cell modules varies significantly, ranging from 1.00E+13 cm^{-3} to 1.00E+22 cm^{-3}. However, it has been noted that this variation does not lead to any noticeable changes in the performance parameters of these solar cells.

3. Results and discussion

The efficient power conversion (PCE) of SnS-based solar cells is shown in this table both before and after escalation.

Table 2. Assessment of power conversion efficiency (PCE) for SnS-based solar cells: optimization effects

SnS-based Solar Cell Models	PCE(%) before optimization	PCE(%) after optimization
Right-contact(front)/TCO/PCBM/SnS/$CuSbS_2$/Left contact(back)	27.94	31.26
Right-contact(front)/TCO/ZnO/SnS/NiO/Left contact(back)	27.95	31.12

Several photovoltaic solar cell (PSC) models were developed and simulated for this investigation. The results, as shown in the table, indicate improved performance characteristics following optimization. Consequently, the models created in this study can be utilized for future research and commercialization.

Table 3. Comparison of established models with the current model in this research.

Models	Methods	Voc(V)	Jsc(mA/cm^2)	FF(%)	PCE(%)	References
Mo/p-SnS/n-SnS/WL	Simulation	0.756	34.9	84.4	22.3	[11]
ZnO/CdS/SnS/NiO/Au	Simulation	0.904	34.20	86.97	26.92	[2]
ITO/CeO_2/SnS/Spiro-OMeTAD/Mo	Simulation	0.887	33.74	85.61	25.65	[4]
TCO/PCBM/SnS/$CuSbS_2$/Left contact(back)	Simulation	1.11	34.23	82.37	31.26	[Present work]
TCO/ZnO/SnS/NiO/Left contact(back)	Simulation	1.09	35.66	82.06	31.12	[Present work]

Current-voltage performance analysis

The figures provide a comparison of the current-voltage characteristics for the two solar cell designs' optimized final model and the starting model.

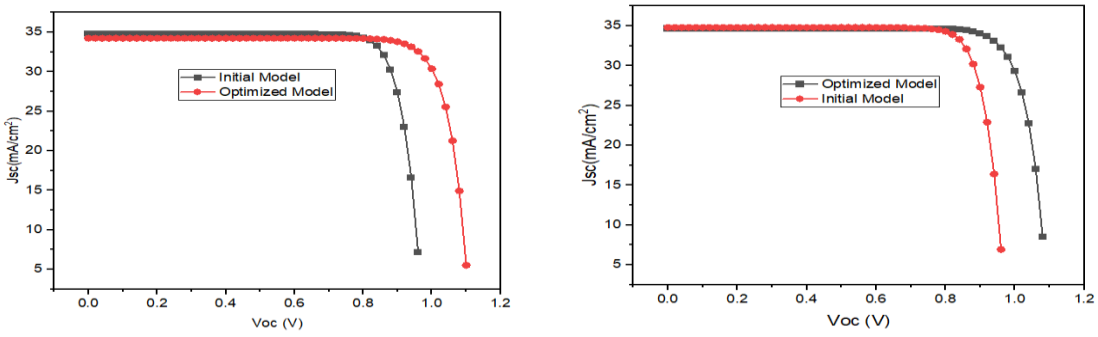


Fig. 7. J-V characteristic curve comparison between the initial and the final optimized models

Comparison of Shockley-Queisser (SQ) limit

The Shockley-Queisser limit represents the theoretical upper bound on the efficiency achievable by a solar cell. The initial computation was conducted by Hans Queisser and William Shockley. The determination of the Shockley-Queisser limit involves the measurement of the amount of electrical energy extracted per incoming photon [12].

Based on the analysis, it can be determined that the upper limit for solar conversion efficiency is around 33.7% [13]. With values of 31.26% and 31.12%, respectively, the two improved solar cells in this work have power conversion efficiencies that fall under the Shockley-Queisser (SQ) limit.

4. Conclusions

In order to determine the optimal material combinations for absorber layers, hole transport layers (HTLs), and electron transport layers (ETLs) in SnS-based solar cells, a thorough analysis was carried out in this work. Tin monosulfide (SnS) was selected as the absorber layer material, paired with various ETLs and HTLs. A detailed simulation was performed, examining numerous unique models. Among the models analyzed, the cell configurations of Right contact (front)/TCO/PCBM/SnS/$CuSbS_2$/Left contact (back) and Right contact (front)/TCO/ZnO/SnS/NiO/Left contact (back) exhibited the highest efficiencies, achieving values of 31.26% and 31.12%, respectively. These findings suggest that the optimal material combinations have significant potential for enhancing efficiency and long-term stability in solar cells. This research lays a solid foundation for future advancements in photovoltaics and contributes to ongoing efforts to harness renewable energy sources for sustainable development.

5. Acknowledgement

For cooperation with the SCAPS-1D simulation program, the researchers of this paper are grateful to Prof. Marc Burgelman of the Department of Electronics and Information Systems at the University of Gent, Belgium.

6. References

[1] A. Hosen and S. Rashel Al Ahmed, “Performance analysis of SnS solar cell with a hole transport layer based on experimentally extracted device parameters.” [Online]. Available: https://ssrn.com/abstract=3987692

[2] A. Umar *et al.*, “Modeling and Simulation of Tin Sulfide (SnS)-Based Solar Cell Using ZnO as Transparent Conductive Oxide (TCO) and NiO as Hole Transport Layer (HTL),” *Micromachines (Basel)*, vol. 13, no. 12, Dec. 2022, doi: 10.3390/mi13122073.

[3] J. A. Andrade-Arvizu, M. Courel-Piedrahita, and O. Vigil-Galán, “SnS-based thin film solar cells: perspectives over the last 25 years,” *Journal of Materials Science: Materials in Electronics*, vol. 26, no. 7, pp. 4541–4556, Jul. 2015, doi: 10.1007/s10854-015-3050-z.

[4] P. Tiwari *et al.*, “Design and Simulation of Efficient SnS-Based Solar Cell Using Spiro-OMeTAD as Hole Transport Layer,” *Nanomaterials*, vol. 12, no. 14, Jul. 2022, doi: 10.3390/nano12142506.

[5] F. Hazeghi and S. M. B. Ghorashi, “Simulation of perovskite solar cells by using CuSCN as an inorganic hole-transport material,” *Mater Res Express*, vol. 6, no. 9, Jul. 2019, doi: 10.1088/2053-1591/ab2f1b.

[6] A. K. Pankaj and S. P. Gangwar, “Optimization of Conversion Efficiency of Perovskite Solar Cell using Cu 2 O and CuI as Hole Transport Layer,” vol. 17, no. 1, pp. 24–33, 2022, doi: 10.9790/2834-1701012433.

[7] P. Tiwari *et al.*, “Design and Simulation of Efficient SnS-Based Solar Cell Using Spiro-OMeTAD as Hole Transport Layer,” *Nanomaterials*, vol. 12, no. 14, Jul. 2022, doi: 10.3390/nano12142506.

[8] Institute of Electrical and Electronics Engineers, Fla. IEEE Photovoltaic Specialist Conference 42 2015.06.14-19 Tampa, Fla. IEEE Photovoltaic Specialists Conference 42 2015.06.14-19 Tampa, and Fla. PVSC 42 2015.06.14-19 Tampa, *2015 IEEE 42nd Photovoltaic Specialist Conference (PVSC) 14-19 June 2015, New Orleans, LA*.

[9] A. Benami, T. Ouslimane, L. Et-taya, and A. Sohani, “Comparison of the Effects of ZnO and TiO2 on the Performance of Perovskite Solar Cells via SCAPS-1D Software Package,” *Journal of Nano- and Electronic Physics*, vol. 14, no. 1, 2022, doi: 10.21272/jnep.14(1).01033.

[10] R. Teimouri and R. Mohammadpour, “Potential application of CuSbS2 as the hole transport material in perovskite solar cell: A simulation study,” *Superlattices Microstruct*, vol. 118, pp. 116–122, Jun. 2018, doi: 10.1016/j.spmi.2018.03.079.

[11] S. Kancharla and D. K. Kaushik, “Optimization of electrical and optical properties of tin sulfide for thin film photovoltaics using SCAPS,” in *Journal of Physics: Conference Series*, Institute of Physics Publishing, Jun. 2020. doi: 10.1088/1742-6596/1531/1/012016.

[12] “https://www.universitywafer.com/what-is-the-shockley-queisser-limit.html.”

[13] K. Wang *et al.*, “Overcoming Shockley-Queisser limit using halide perovskite platform?,” Apr. 20, 2022, *Cell Press*. doi: 10.1016/j.joule.2022.01.009.